Old Drug Scaffold, New Activity: Thalidomide-Correlated Compounds Exert Different Effects on Breast Cancer Cell Growth and Progression

Domenico Iacopetta[+,a] Alessia Carocci[+,b] Maria Stefania Sinicropi,*[a] Alessia Catalano,*[b] Giovanni Lentini,[b] Jessica Ceramella,[a] Rosita Curcio,[a] and Maria Cristina Caroleo[a]

Thalidomide was first used for relief of morning sickness in pregnant women and then withdrawn from the market because of its dramatic effects on normal fetal development. Over the last decades, it has been used successfully for the treatment of several pathologies, including cancer. Many analogues with improved activity have been synthesized and tested. Herein we report some effects on the growth and progression of MCF-7 and MDA-MB-231 breast cancer cells by a small series of thalidomide-correlated compounds, which are very effective at inducing cancer cell death by triggering TNFα-mediated apoptosis. The most active compounds are able to drastically reduce the migration of breast cancer cells by regulation of the two major proteins involved in epithelial–mesenchymal transition (EMT): vimentin and E-cadherin. Moreover, these compounds diminish the intracellular biosynthesis of vascular endothelial growth factor (VEGF), which is primarily involved in the promotion of angiogenesis, sustaining tumor progression. The multiple features of these compounds that act on various key points of the tumorigenesis process make them good candidates for preclinical studies.

Introduction

Thalidomide is a glutamic acid derivative that was first synthesized in Germany in 1954 and marketed in 46 countries in the late 1950s and early 1960s for relief of morning sickness in pregnant women.[1] However, a massive increase in the number of newborns with severe malformations (deafness, blindness, limb growth defects) was registered after the use of thalidomide, and the drug was subsequently withdrawn in 1962.[2] Over the last few decades, interest in this old drug has been renewed, given its efficacy in several important diseases, such as erythema nodosum leprosum,[3] multiple myeloma,[4] breast cancer,[5] refractory Crohn's disease,[6] and HIV-related diseases.[7] It has become clearer that thalidomide has multifaceted properties, leading many research groups to synthesize several derivatives and to study their effects, mostly in cancer research. The growth and progression of cancers require fundamental changes, for example, in energy metabolism pathways, nutrient uptake, and in several other factors, leading to phenotypic heterogeneity within subpopulations of cancer cells.[8,9] These changes allow a greater capacity to grow under suboptimal micro-environmental conditions such as nutrient depletion and hypoxia.[10] ■■Rewording OK?■■

In 1994, D'Amato et al.[11] reported that thalidomide is able to inhibit angiogenesis induced in a rabbit cornea model, shedding light on the antiangiogenic role responsible for teratogenicity. Remarkably, angiogenesis is essential for cancer growth, progression, and metastasis; amongst the pro-angiogenic factors, vascular endothelial growth factor (VEGF) plays a key role because of its up-regulation in tumors.[12] Furthermore, much published data have shown that thalidomide inhibits the production of tumor necrosis factor α (TNFα), which plays a dual role in cell proliferation, stimulating tumor cell growth or inducing cancer cell death.[13] Starting from thalidomide as a lead compound, several analogues have been developed, sharing and augmenting the antiproliferative, antiangiogenic, and TNFα-reducing properties of the parent compound.[14–18]

Another interesting thalidomide effect is its ability to inhibit the epithelial–mesenchymal transition (EMT), a dynamic process enabling polarized epithelial cells to assume a mesenchymal phenotype with enhanced migratory and invasive capabilities.[19] EMT is associated with the early stages of carcinogenesis, cancer invasion and recurrence, and is characterized by a decrease in epithelial cell-junction proteins, including E-cadherin, α-catenin, claudins, and occludin, combined with an increased expression of mesenchymal markers such as N-cadherin, vimentin, and fibronectin. In this context, it is of great interest to design and synthesize thalidomide analogues that are able to exert multiple effects on cancer cell proliferation.[20,21]

Herein we report the antitumor activity of some thalidomide analogues and correlated compounds (Figure 1), which are able to trigger cell death by TNFα-mediated apoptosis in two breast cancer cell lines, MCF-7 and MDA-MB-231, without af-

[a] Dr. D. Iacopetta,[+] Prof. M. S. Sinicropi, Dr. J. Ceramella, Dr. R. Curcio, Prof. M. C. Caroleo
Department of Pharmacy, Health and Nutritional Sciences, University of Calabria, 87036, Arcavacata di Rende (Italy)
E-mail: s.sinicropi@unical.it
[b] Dr. A. Carocci,[+] Dr. A. Catalano, Prof. G. Lentini
Department of Pharmacy-Drug Sciences, University of Bari "Aldo Moro", 70126, Bari (Italy)
E-mail: alessia.catalano@uniba.it
[+] These authors contributed equally to this work.

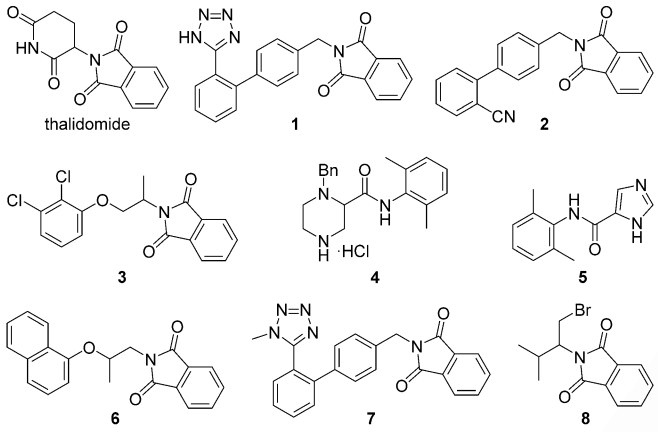

Figure 1. Structures of thalidomide and correlated compounds.

fecting the proliferation of non-tumor MCF-10A cells. Moreover, some of these compounds are able to decrease cancer cell migration, regulating the expression of two important proteins involved in EMT, namely E-cadherin and vimentin. We show that these compounds have better activity and be more effective at interfering with various breast tumor targets, thereby offering a viable alternative in cancer treatment.■■Rewording OK?■■

Chemistry

Compounds **1**, **7**,[22] **2**,[23] **3**, and **6**[24] (Figure 1) were prepared as described elsewhere. Chiral compounds (**3**, **4**, **6**, **8**) were prepared in their racemic forms. Compound **4** was prepared as shown in Scheme 1. Compound **10** was readily prepared by

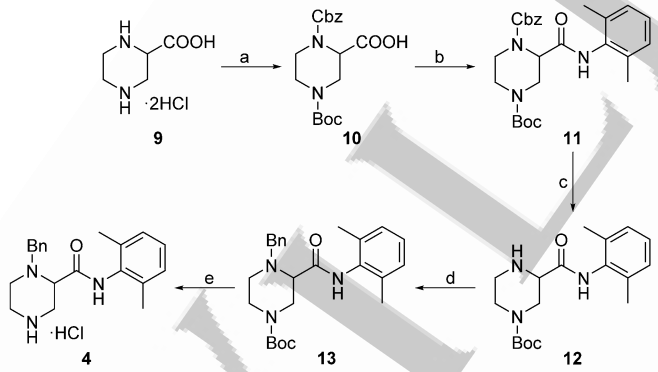

Scheme 1. Synthesis of compound **4**. Reagents and conditions: a) Boc-ON, benzyl chloroformate, dioxane/H_2O, RT;■■Reaction time?■■ b) 2,6-dimethylaniline, IIDQ, Et_3N, $CHCl_3$, reflux, 6 h; c) Et_3SiH, $PdCl_2$, Et_3N, CH_2Cl_2, reflux, 3 h; d) BnBr, K_2CO_3, dioxane/H_2O, 70 °C, 45 min; e) HCl, anhyd. Et_2O, RT, 15 min.■■Reaction times added; OK?■■

the selective Boc-group protection of piperazine-2-carboxylic acid (**9**) at the 4-position, followed by Cbz-group protection at the 1-position.[25] Compound **10** was then treated with 2,6-dimethylaniline in the presence of 2-isobutoxy-1-isobutoxycarbonyl-1,2-diihydroquinoline (IIDQ) to afford the corresponding carboxamide **11**.[26] Selective Cbz deprotection of **11** with triethylsilane and palladium chloride[27] gave **12**, which was converted into the *N*-benzyl derivative **13** by reaction with benzyl bromide.[28] Boc deprotection of **13** and conversion of the resulting amine into the corresponding hydrochloride salt was performed with gaseous HCl as previously described.[29] Compound **5** was synthesized as shown in Scheme 2 by reacting

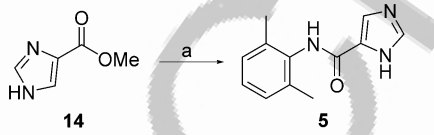

Scheme 2. Synthesis of compound **5**. Reagents and conditions: a) 2,6-dimethylaniline, NaH, dry dioxane/dry DMF, reflux, 5 h.■■Reaction time added; OK?■■

methyl imidazole-4-carboxylate (**14**) with 2,6-dimethylaniline according to a published procedure.[30] Compound **8** was synthesized as illustrated in Scheme 3. Amino alcohol **15** was protected with phthalic anhydride[31] to give the phthalimido alcohol **16**, which was converted into the corresponding bromo derivative **8** by treatment with PBr_3.

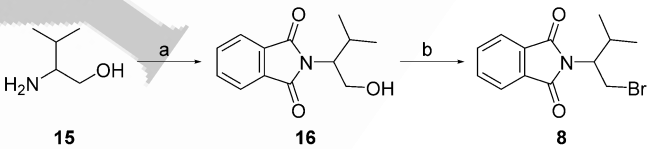

Scheme 3. Synthesis of compound **8**. Reagents and conditions: a) phthalic anhydride, Et_3N, toluene, reflux, 3 h; b) PBr_3, 0 °C, 2 h, then RT, 6 h.■■Reaction times added; OK?■■

Results and Discussion

Antiproliferative activity

Thalidomide analogues were evaluated for their antiproliferative activities against two human breast cancer cell lines, namely estrogen receptor (ER)-positive (ER+) MCF-7■■′MCF-7′ here; OK?■■ and triple-negative (ER^-, PR^-, and HER-2/Neu unamplified) MDA-MB-231 cells.[32] Cells were subjected to continuous exposure to the test compounds for 72 h, after which their viability was measured by 3-(4,5-dimethylthiazol-2-y1)-2,5-diphenyltetrazolium (MTT) test.[33,34] Thalidomide was used as reference in these assays. The IC_{50} values, i.e., compound concentrations producing 50% growth inhibition, are listed in Table 1. As shown, thalidomide exerted only very low antitumor activity in both cell lines tested, showing slight effects only at doses higher than 500 μM, whereas very impressive activity was observed with the synthesized compounds. In particular, compounds **3** and **8** were found to be the most active, with IC_{50} values of 47 ± 1 and 40.3 ± 0.8 μM toward MCF-7 cells and 56.5 ± 1.3 and 37.2 ± 1.0 μM toward MDA-MB-213 cells, respectively. The other compounds also showed interesting anti-

Table 1. IC_{50} values of thalidomide and compounds **1**–**8**.

Compound	IC_{50} [μM][a]		
	MCF-7	MDA-MB-231	MCF-10A
thalidomide	360 ± 2	413 ± 2	> 500
1	293.8 ± 1.0	> 500	> 500
2	99.6 ± 1.2	165.5 ± 1.8	> 500
3	47 ± 1	56.5 ± 1.3	> 500
4	204.8 ± 0.7	119.3 ± 1.8	> 500
5	> 500	> 500	> 500
6	302.6 ± 2.1	151.9 ± 1.6	> 500
7	57.3 ± 2.2	80.9 ± 2.2	> 500
8	40.3 ± 0.8	37.2 ± 1.0	> 500

[a] Values are the mean ± SD of three independent experiments performed in triplicate.

proliferative effects, albeit to a lesser extent (Table 1). Once established that our compounds possess improved antitumor activity with respect to thalidomide, we tested all the considered compounds on nonmalignant breast epithelial cells (MCF-10A) to determine any cytotoxic effects. We found that none of the compounds produce toxic effects on the viability of normal breast epithelial cells up to 500 μM. The improved capacity of our compounds to affect the proliferation of MCF-7 cells and, most importantly, the highly aggressive and metastatic MDA-MB-231 cell line, without affecting non-tumor MCF-10A breast epithelial cells, prompted us to investigate the properties of the most active compounds in greater detail.

Breast cancer cell death by TNFα-mediated apoptosis

In previous reports, thalidomide was found to suppress the expression of TNFα mRNA.[35] In this regard, published data have clarified the complex interplay between TNFα and apoptosis, highlighting that TNFα can promote apoptotic cell death through the activation of several caspases and by mitochondrial damage, a pattern known as the extrinsic apoptotic pathway. We therefore investigated the ability of compounds **3** and **8** to modulate TNFα cell levels by immunofluorescence analysis. MCF-7 cells were exposed for 24 h to the two different compounds at concentrations equal to their respective IC_{50} values. Cells were then processed for immunofluorescence assays using an antibody raised against TNFα; vehicle-treated cells were used as a control. Immunofluorescence analysis of MCF-7 cells treated with compounds **3** and **8** revealed a three- and two-fold increase in TNFα expression, respectively (Figure 2). Furthermore, 2-(4-amidinophenyl)-6-indolecarbamidine dihydrochloride (DAPI) staining of the same samples highlighted nuclei containing condensed DNA, frequently associated with apoptosis. It is known that the activation of the extrinsic apoptotic pathway implies increased mitochondrial permeability, followed by the cytosolic release of cytochrome *c*, a small protein associated with the inner membrane of intact mitochondria, which may act as an apoptogenic factor.[36] Therefore, we further investigated the subcellular localization of cytochrome *c* in MCF-7 cells treated with compounds **3** or **8**, using an antibody raised against cytochrome *c* (Figure 3 A).

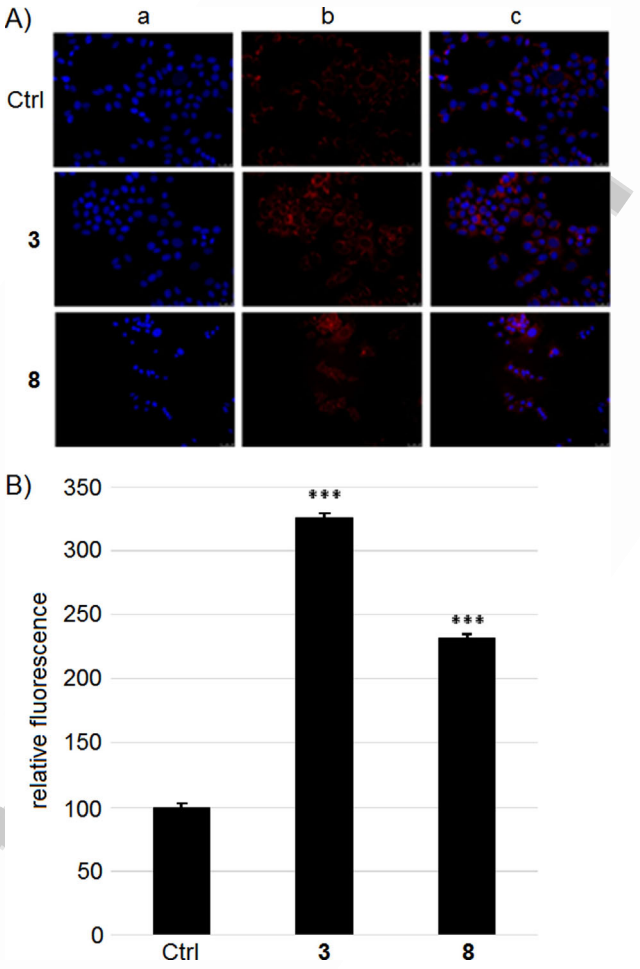

Figure 2. A) Immunofluorescence analysis of TNFα levels in MCF-7 cells. Cells were treated for 24 h with compounds **3** and **8** or vehicle (Ctrl), then processed as described in the Experimental Section. Images were acquired at 20× magnification. a) DAPI, b) Alexa Fluor® 568, c) overlay; images are representative of three separate experiments. B) Fluorescence quantification; ***$p < 0.001$.

Remarkably, cytochrome *c* was released in the cytosol of the treated cells, as is evidenced by the increased and diffused fluorescence (Figure 3), whereas in vehicle-treated cells, it is still localized in the mitochondrial network. Moreover, a terminal deoxynucleotidyl transferase dUTP nick end labeling (TUNEL) assay conducted on MCF-7 cells treated for 24 h with compounds **3** or **8** revealed green fluorescence in the cell nuclei, which indicates DNA fragmentation correlated with the apoptotic process (Figure 4). Taken together, our data highlight that compounds **3** and **8** are able to promote breast cancer cell death by increasing TNFα synthesis, which, in turn, promotes cytochrome *c* release from mitochondria, and therefore, apoptosis.

Effects of compounds 1–8 on breast cancer cell migration

We tested the ability of compounds **1**–**8** to affect the migration of MCF-7 and MDA-MB-231 cells by using a simple, low-cost, and well-developed in vitro method: the wound-healing

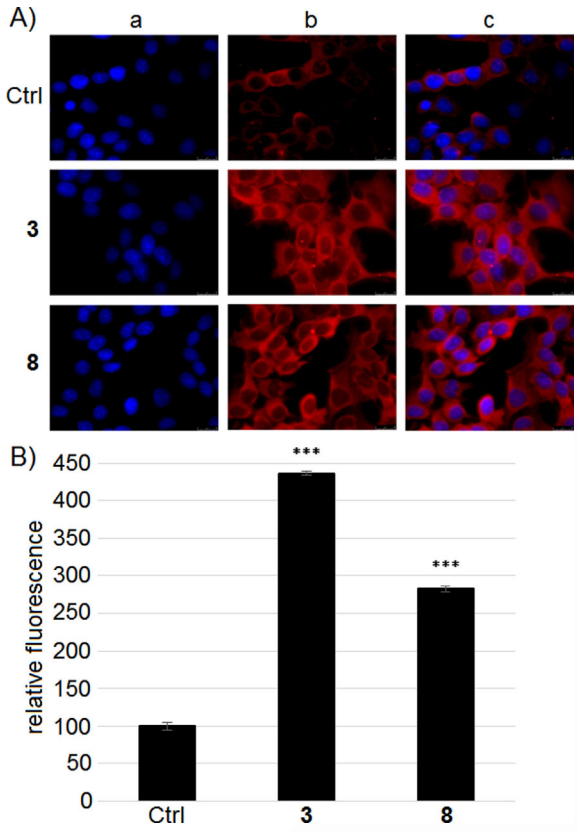

Figure 3. A) Immunofluorescence analysis of cytochrome *c*. MCF-7 cells were treated for 24 h with compounds **3** or **8**, or with vehicle (Ctrl). Images were acquired at 63× magnification. a) DAPI, b) Alexa Fluor® 568, c) overlay; images are representative of three separate experiments. B) Fluorescence quantification; ***$p < 0.001$.

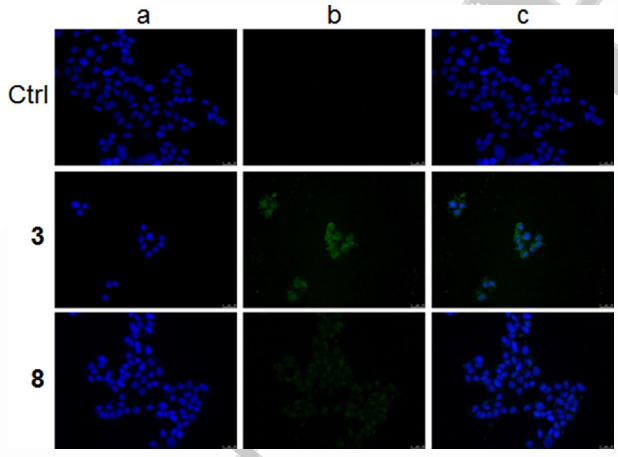

Figure 4. Apoptosis detection by TUNEL assay on MCF-7 breast cancer cells. Cells were treated for 24 h with compounds **3** and **8**, then fixed with cold methanol and subjected to the TUNEL procedure. Cells were then washed, dyed with DAPI, and observed and imaged under an inverted fluorescence microscope (20× magnification). a) CF™488A, b) DAPI, c) overlay; representative fields are shown.

assay. Cells were plated and cultured to form a monolayer, then scratched to form a wound (see Experimental Section) and treated with compounds **1**–**8** at concentrations corresponding to their respective IC_{50} values (Table 1) for 48 and 72 h, for MDA-MB-231 and MCF-7 cells, respectively. These different endpoint times were experimentally determined, considering that MDA-MB-231 cells have a higher growth rate than MCF-7 cells and tend to give greater metastases in vivo.[37] In MCF-7 cells compounds **2**, **3**, **7**, and **8** produced higher effects, preventing total wound closure at percentages of ~52, 77, 72, and 69% (Figure 5 A). In MDA-MB-231 cells, the same compounds produced a significant lack of total wound closure (~11, 25, 27, and 25%, respectively); however, in contrast to MCF-7 cells, compound **6** exhibited an impressive effect in preventing wound closure: ~32% (Figure 5 B). The other compounds had no significant effects in such experiments. In both breast cancer cell lines, compound **2** was the most effective in preventing wound closure (Figure 3) with respect to the other active compounds, but it possesses lower efficacy in decreasing cell viability, as demonstrated in our previous experiments (Table 1). Overall, our data highlight that compounds **3** and **8** have good activity in diminishing cancer cell migration (Figures 5 and 6), together with the lowest IC_{50} values (Table 1). Thus, we chose these two compounds for further investigations.

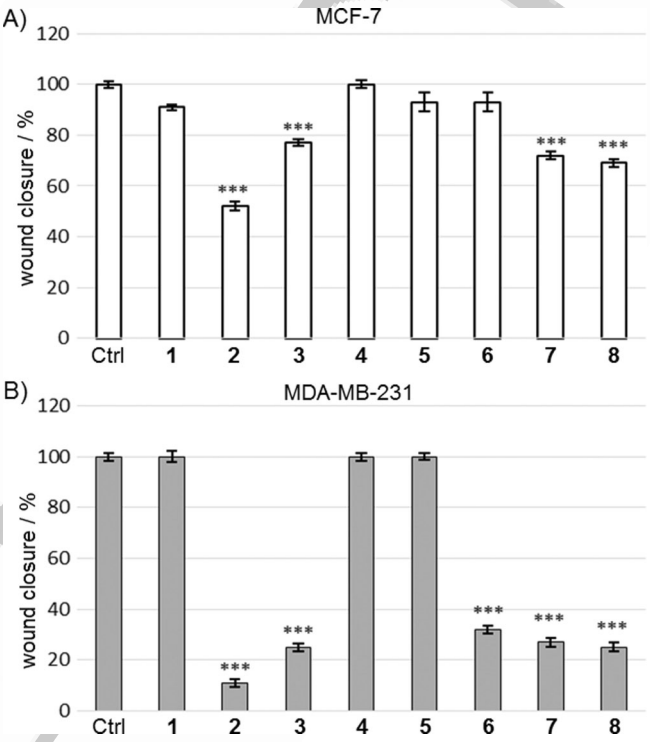

Figure 5. Wound-healing assay conducted on A) MCF-7 and B) MDA-MB-231 cells treated with compounds **1**–**8**. Wound closure was monitored by recording the area of the cell-free wound at 0 and 72 h for MCF-7 and at 0 and 48 h for MDA-MB-231, by the use of an inverted microscope. The wound-healing effect was estimated as the percentage of wound closure calculated as reported in the Experimental Section. Vehicle-treated (Ctrl) cells were used as a control; ***$p < 0.001$.

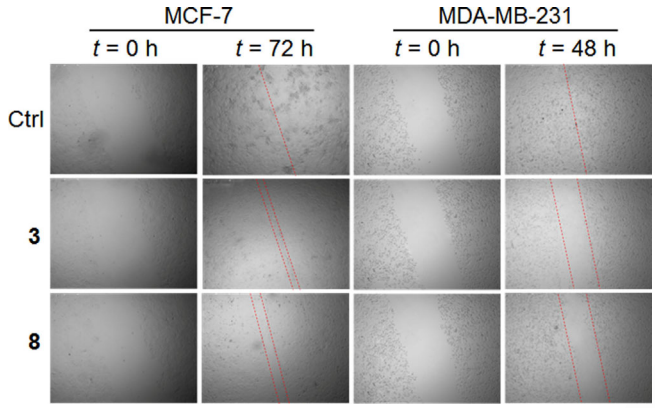

Figure 6. Wound-healing assay conducted on A) MCF-7 and B) MDA-MB-231 cells plated on six-well plates and treated with compounds **3** or **8** and vehicle (Ctrl). Wound closure was monitored at 0 and 72 h for MCF-7 and at 0 and 48 h for MDA-MB-231, by the use of an inverted microscope (5× magnification). Dotted red lines define the areas that lack cells.

Compounds 3 and 8 hamper EMT, decreasing breast cancer cell invasiveness

We first tried to better understand the role of compounds **3** and **8** in breast cancer cell invasion. Indeed, during EMT, malignant cells reorganize their cytoskeleton, expressing mesenchymal markers as vimentin, and lose intercellular adhesion molecules such as E-cadherin, which is considered a diagnostic biomarker in breast cancer.[38] In this regard, we tested the ability of compounds **3** and **8** to modulate vimentin and E-cadherin levels in MCF-7 cells. Cells were exposed to the compounds for 24 h, used at concentrations equal to their IC_{50} values, processed, and subjected to immunofluorescence analysis using antibodies against vimentin and E-cadherin. Vehicle-treated cells were used as a control. Immunofluorescence microscopy analysis showed that both compounds **3** and **8** strongly decreased vimentin levels (Figure 7). At the same time, they significantly increased E-cadherin levels (Figure 8), mostly at the cytoplasmic membrane, where cell–cell interactions occur. These data indicate that compounds **3** and **8** may play a role in inhibiting the EMT process through regulation of vimentin and E-cadherin expression, which are mainly involved in cancer cell invasion and metastasis.

Compounds 3 and 8 can inhibit VEGF expression in breast cancer cells

Thalidomide is known to be a potent inhibitor of angiogenesis, an essential process in cancer cell proliferation, extracellular matrix invasion, and metastasis. In 2006, Komorowski et al.[39] reported that this drug can inhibit VEGF secretion in a human endothelial cell line, decreasing neovascularization; VEGF can act as an autocrine or paracrine factor in the invasiveness of several cell types via receptor binding. On this basis, through immunofluorescence studies we tested whether compounds **3** and **8** could interfere with VEGF expression in MCF-7 cells. MCF-7 cells were thus treated with compounds **3** or **8** at their own IC_{50} values for 24 h, and then subjected to immunofluorescence staining using an antibody raised against VEGF (Figure 9A). In such experiments, vehicle-treated cells were used as a control (Ctrl). Interestingly, the fluorescent cytoplasmic signal that is correlated with the presence of VEGF was markedly decreased in MCF-7 cells treated with both compounds **3** and **8**, with respect to the vehicle-treated cells (Figure 9), indicating interference with VEGF biosynthesis. This feature has also been correlated with apoptosis induction in ER-positive and triple-negative breast cancer cells, as previously reported.[40] Additionally, in MCF-7 cells treated with compound **8**, the decrease of VEGF-associated fluorescence is accompanied by an evident change in subcellular localization (Figure 9A, white arrows), which is evidently no longer localized in the perinuclear area, as in the vehicle-treated cells, but is also diffused in the nuclei. This difference could indicate decreased biosynthesis at the endoplasmic reticulum network and an interaction with nuclear receptors. VEGF nuclear accumulation may play several and still poorly understood roles; however, Li and Keller[41] suggested a role in coagulation and fibrinolysis pathways, affecting vascular endothelial cellular physiology independent of its growth stimulation. The latter observation contrasts with the results obtained by scratch and MTT assays,

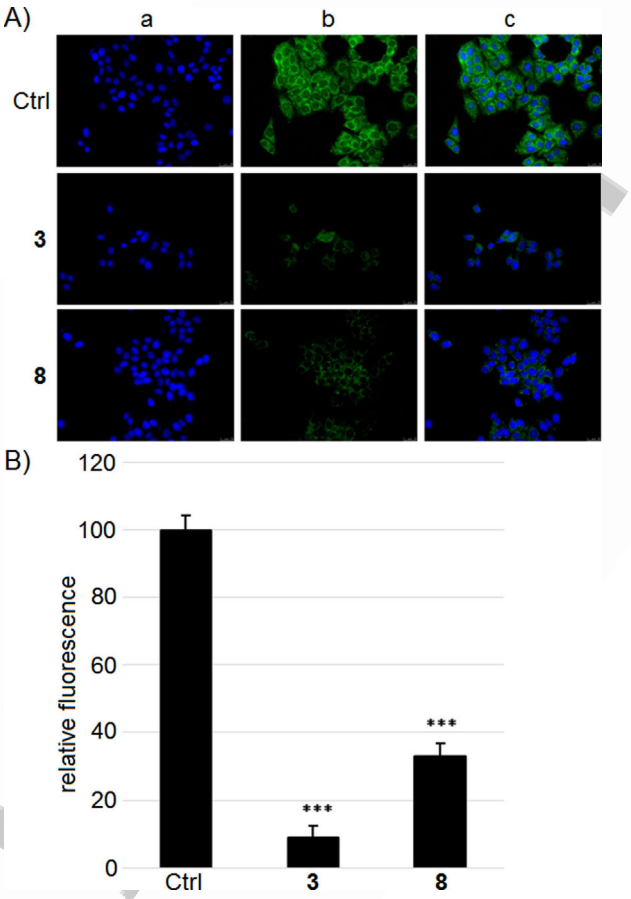

Figure 7. Immunofluorescence analysis of vimentin. A) MCF-7 cells were treated for 24 h with compounds **3**, **8**, or vehicle (Ctrl). Images were acquired at 20× magnification. a) DAPI, b) Alexa Fluor® 488, c) overlay; images are representative of three separate experiments. B) Fluorescence quantification, ***$p < 0.001$.

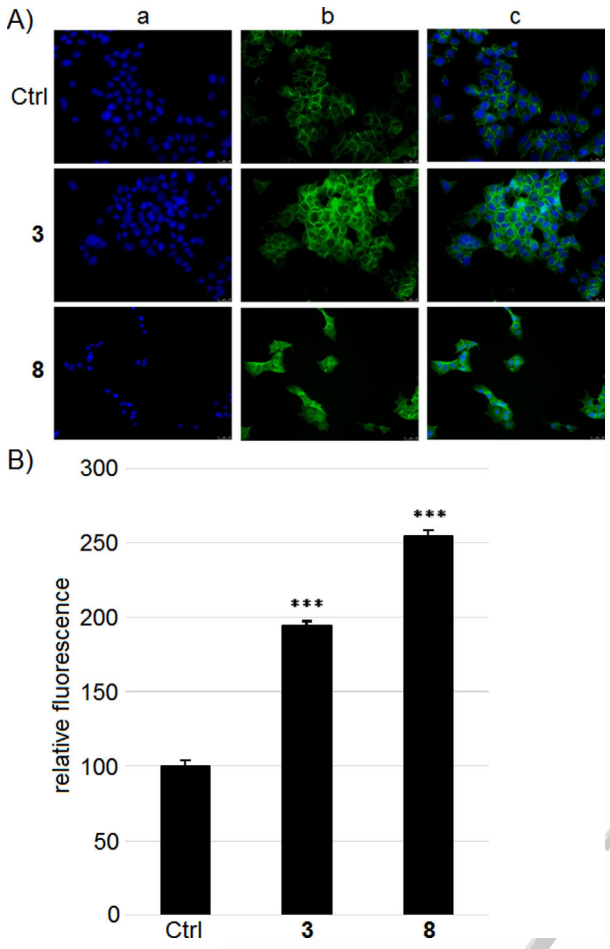

Figure 8. Immunofluorescence analysis of E-cadherin. A) MCF-7 cells were treated for 24 h with compounds **3**, **8**, or vehicle (Ctrl). Images were acquired at 20× magnification. a) DAPI, b) Alexa Fluor® 488, c) overlay; images are representative of three separate experiments. B) Fluorescence quantification, $^{***}p < 0.001$.

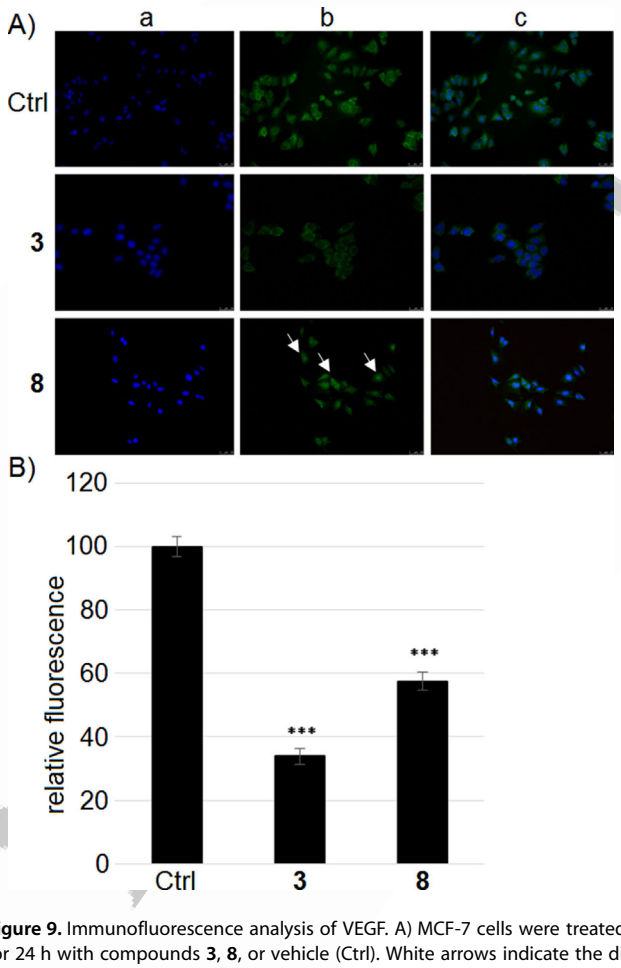

Figure 9. Immunofluorescence analysis of VEGF. A) MCF-7 cells were treated for 24 h with compounds **3**, **8**, or vehicle (Ctrl). White arrows indicate the different subcellular localization of VEGF in MCF-7 cells treated with compound **8**, with respect to the vehicle-treated cells. Images were acquired at 20× magnification. a) DAPI, b) Alexa Fluor® 488, c) overlay; images are representative of three separate experiments. B) Fluorescence quantification, $^{***}p < 0.001$.

but further studies are needed in order to shed light on this feature. In summary, our observations highlight the antiangiogenic potential of these compounds, which is one of the most desired features of drugs used for the treatment of breast cancer.

Conclusions

The library of thalidomide-correlated compounds reported herein consists of three newly synthesized compounds (**4**, **5**, and **8**) and five other previously reported thalidomide analogues (**1**, **2**, **3**, **6**, and **7**). The studied compounds show some interesting properties on breast cancer cells, particularly the ER+ MCF-7 and triple-negative MDA-MB-231 cell lines. Compared with the lead molecule thalidomide, some of these compounds show higher antitumor activity; in particular, compounds **3** and **8** have IC_{50} values nearly ten-fold lower than that of thalidomide. Moreover, no significant cytotoxic effects were observed regarding the viability of MCF-10A normal breast cells.

The antitumor effects have been ascribed to an intracellular increase in TNFα biosynthesis, which we believe is responsible for a protection mechanism (paracrine effect) against the abnormal proliferation of surrounding breast cancer cells. Indeed, this cytokine may trigger the apoptotic process through the mitochondrial pathway, given that a massive release of cytochrome *c* from the mitochondrial compartment into the cytosol was detected by immunofluorescence assays. Cancer cell death by apoptosis has been definitively proven by TUNEL assay. Besides these effects on the viability of breast cancer cells, compounds **3** and **8**, chosen to further investigate other properties, are also able to decrease cancer cell migration and invasion, as demonstrated by wound-healing assays. These features reside in the regulation of two major proteins involved in the EMT—vimentin and E-cadherin—which allow tumor cells to detach from the original site and disseminate through the bloodstream. The inhibition of vimentin biosynthesis and the increase in E-cadherin expression induced by our compounds are very interesting features, making cancer cells less prone to engage in invasion and metastasis. Finally, compounds **3** and **8** may play a role in regulating VEGF expression in breast cancer

cells, given that we observed a decrease in intracellular VEGF levels and a different subcellular localization in cancer cells treated with compound **8**. In this regard, other studies are required to better understand the precise mechanism responsible for the effects observed. However, we believe that these compounds possess great potential because of their multiple properties toward different aspects of breast cancer cell biology. Indeed, besides their selective killing effect on cancer cells, their capacity to interfere with the migration and invasion processes, which are the main cause of death for breast cancer patients, is a very promising property. Lastly, the role played by our compounds in decreasing the levels of VEGF, which is mainly involved in the angiogenesis pathway responsible for promoting cancer survival, completes the range of multiple anticancer properties exerted by our compounds.■■Rewording OK?■■ We are confident that our research will be seminal and will encourage other studies on the design, development, and biological evaluation of thalidomide-correlated compounds.

Experimental Section

Chemistry

All reagents were purchased from Sigma–Aldrich or Lancaster in the highest quality commercially available. Solvents were reagent grade unless otherwise indicated. Yields refer to purified products and were not optimized. The structures of the compounds were confirmed by routine spectrometric analyses. Only spectra for compounds not previously described are given. Melting points were determined on a Gallenkamp melting point apparatus in open glass capillary tubes and are uncorrected. ^{1}H and ^{13}C NMR spectra were recorded on a Varian VX Mercury spectrometer operating at 300 and 75 MHz for ^{1}H and ^{13}C, respectively, or an Agilent 500 MHz operating at 500 and 125 MHz for ^{1}H and ^{13}C, respectively, using $CDCl_3$ and [D_6]DMSO as solvents. Chemical shifts are reported in parts per million [ppm] relative to solvent resonance: $CDCl_3$, $\delta=$ 7.26 ppm (^{1}H NMR) and $\delta=77.0$ ppm (^{13}C NMR); [D_6]DMSO, $\delta=$ 2.48 ppm (^{1}H NMR) and $\delta=39.9$ ppm (^{13}C NMR). *J* values are given in Hz. The following abbreviations are used: s singlet, d doublet, t triplet. Gas chromatography/mass spectrometry (GC–MS) was performed on a Hewlett-Packard 6890-5973 MSD instrument at low resolution. Elemental analyses were performed on a Eurovector Euro EA 3000, analyzer and the data for C, H, N were within $\pm$0.4 of theoretical values (Table S1).■■No supporting information file provided; please clarify?■■ Chromatographic separations were performed on silica gel columns by flash chromatography (Kieselgel 60, 0.040–0.063 mm, Merck, Darmstadt, Germany) as previously described.[42]

***N*-(2,6-Dimethylphenyl)piperazine-1-[(benzyloxy)carbonyl]-4-(*tert*-butoxycarbonyl)piperazine-2-carboxamide (11).** IIDQ (0.27 mL, 0.92 mmol), 2,6-dimethylaniline (0.99 mL, 0.85 mmol) and Et_3N (0.16 mL, 1.15 mmol) were successively added to a stirring solution of compound **10** (0.28 g, 0.77 mmol) in $CHCl_3$ (26 mL). The reaction mixture was heated under reflux for 6 h. The solvent was removed under reduced pressure and the residue, taken up with EtOAc, was washed three times with 2 N HCl, twice with 2 N NaOH, and then dried over anhydrous Na_2SO_4. Flash chromatography (eluent EtOAc/petroleum ether 4:6) of the residue gave 90 mg (25% yield) of **11** as a light-yellow oil: GC–MS (70 eV) *m/z* (%) 367 (<1) [M^+-100], 91 (100).

***tert*-Butyl 3-[(2,6-dimethylphenyl)carbamoyl]piperazine-1-carboxylate (12).** A suspension of compound **11** (80 mg, 0.17 mmol), Et_3SiH (0.11 mL, 0.68 mmol), Et_3N (17 μL, 0.12 mmol), and $PdCl_2$ (9.03 mg, 0.051 mmol) in CH_2Cl_2 (1 mL) was heated at reflux for 3 h. The reaction mixture was quenched with saturated aqueous NH_4Cl and extracted with Et_2O■■Replaced 'ether' here; OK?■■ several times. The combined organic phases were washed with H_2O and then brine, dried, and concentrated in vacuo to give 45 mg (79%) of a light-yellow oil: GC–MS (70 eV) *m/z* (%) 333 (3) [M^+], 129 (100).

***tert*-Butyl 4-benzyl-3-(2,6-dimethylphenylcarbamoyl)piperazine-1-carboxylate (13).** To a stirring solution of compound **12** (0.15 g, 0.45 mmol) in dioxane (8 mL), a solution of K_2CO_3 (0.18 g, 1.30 mmol) in H_2O (8 mL) was added. The reaction mixture was heated at 70 °C, and then benzyl bromide (63 μL, 0.53 mmol) was added dropwise. The heating was continued for 45 min. The dioxane was then removed under reduced pressure and the aqueous residue was taken up with EtOAc and extracted with 2 N HCl. The aqueous phase was made alkaline with 2 N NaOH and extracted twice with EtOAc. The combined organic layers were dried over anhydrous Na_2SO_4 and concentrated under vacuum to give 90 mg (47%) of a yellow oil: GC–MS (70 eV) *m/z* (%) 323 (2) [M^+-100], 175 (100).

1-Benzyl-*N*-(2,6-dimethylphenyl)piperazine-2-carboxamide hydrochloride (4·HCl). Compound **4** as hydrochloride salt was obtained by saturating a solution of compound **13** in anhydrous Et_2O with gaseous HCl and stirring it at room temperature for 15 min. Removal of the solvent under reduced pressure gave a white solid (67%) which was recrystallized from EtOH/Et_2O to afford white crystals: mp: 235–237 °C (abs. EtOH/Et_2O); Anal. calcd for $C_{12}H_{13}N_3O$: C 65.70, H 7.90, N 11.49, found: C 65.35, H 7.68, N 11.22.

***N*-(2,6-Dimethylphenyl)-1*H*-imidazole-4-carboxamide (5).** To a stirring suspension of 60% NaH (0.27 g, 6.67 mmol) in dry dioxane (10 mL) under N_2 atmosphere, 2,6-dimethylaniline (0.72 g, 5.95 mmol) was added and the mixture brought to reflux. Then, a solution of methyl imidazole-4-carboxylate (**14**, 0.30 g, 2.30 mmol) in dry DMF (13 mL) was added dropwise in an ice bath. After 5 h the mixture was poured into ice and extracted with EtOAc. The organic layer was then evaporated in vacuo. Purification by column chromatography gave 0.26 g (53%) of **5** as a light-yellow solid: mp: 212–214 °C; ^{1}H NMR (500 MHz, [D_6]DMSO): $\delta=$ 2.18 (s, 6H, CH_3), 3.77 (br s, 1H, N*H*), 7.05–7.15 (m, 3H, Ar), 8.57 (s, 1H, Ar), 9.18 (s, 1H, Ar), 10.5 ppm (s, exch D_2O, 1H, N*H*); ^{13}C NMR (125 MHz, [D_6]DMSO): $\delta=$18.6 (2C), 121.6 (1C), 127.6 (1C), 128.2 (1C), 128.3 (2C), 134.2 (2C), 135.9 (1C), 136.5 (1C), 156.1 ppm (1C); GC–MS (70 eV) *m/z* (%) 215 (27) [M^+], 121 (100); Anal. calcd for $C_{12}H_{13}N_3O$: C 66.96, H 6.09, N 19.52, found: C 66.62, H 5.89, N 19.20.

2-(1-Hydroxy-3-methylbutan-2-yl)-1*H*-isoindole-1,3(2*H*)-dione (16). A mixture of 2-amino-3-methylbutan-1-ol **15** (5 mmol), phthalic anhydride (5 mmol) and Et_3N (0.5 mmol) in 10 mL of toluene was heated under reflux in a flask fitted with a Dean–Stark tube for 3 h. During this period, the temperature of the oil bath was maintained at ~130 °C, and H_2O separated out. All volatile matter was then evaporated under vacuum, and the solid residue was taken up with EtOAc and washed with 2 N HCl, $NaHCO_3$, and H_2O. The organic phase was dried (Na_2SO_4) and concentrated under vacuum to give 0.56 g of **16** as a yellow oil (48%): GC–MS (70 eV) *m/z* (%) 233 (2) [M^+], 202 (100).

2-(1-Bromo-3-methylbutan-2-yl)-1*H*-isoindole-1,3(2*H*)-dione (8). PBr_3 (1.7 mmol) was carefully added to **16** (1.5 mmol) at 0 °C. The

reaction mixture was stirred for 2 h at 0 °C and for 6 h at room temperature, then poured onto ice and extracted with EtOAc. The organic layer was washed with brine, dried over Na_2SO_4, and the solvent was evaporated in vacuo to give a pale-yellow oily residue. Purification by column chromatography (eluent EtOAc/hexane 2:8) gave 0.30 g (66%) of **8** as a white solid: ^{1}H NMR (500 MHz, $CDCl_3$): $\delta = 0.91$ (d, $J = 6.4$ Hz, 3H, CH_3), 1.08 (d, $J = 6.4$ Hz, 3H, CH_3), 2.36–2.46 (m, 1H, $CHCH_3$), 3.75–3.83 (m, 1H, CHN), 4.10–4.22 (m, 2H, CH_2), 7.68–7.78 (m, 2H, Ar), 7.82–7.90 ppm (m, 2H, Ar); ^{13}C NMR (125 MHz, $CDCl_3$): $\delta = 20.3$ (1C), 20.4 (1C), 30.4 (1C), 31.5 (1C), 59.6 (1C), 123.4 (2C), 131.5 (2C), 134.1 (2C), 168.4 ppm (2C); GC–MS (70 eV) *m/z* (%) 296 (1) [M^+], 252 (100); anal. calcd for $C_{13}H_{14}N_2OBr$: C 52.72, H 4.76, N 4.73, found: C 52.73, H 4.99, N 4.43.

Biology

Cell culture. The three cell lines used in this work were purchased from American Type Culture Collection (ATCC, Manassas, VA, USA). MCF-7 human breast cancer cells, estrogen receptor (ER)-positive, were maintained in Dulbecco's modified Eagle's medium/nutrient mixture Ham F-12 (DMEM/F12), supplemented with 10% fetal bovine serum (FBS) and 100 U mL^{-1} penicillin/streptomycin, as previously described.[43] MCF-10A human mammary epithelial cells, were cultured in DMEM/F12 medium, supplemented with 5% horse serum (HS; Eurobio, Les Ullis, Cedex, France), 100 U mL^{-1} penicillin/streptomycin, 0.5 mg mL^{-1} hydrocortisone, 20 ng mL^{-1} human epidermal growth factor (hEGF), 10 μg mL^{-1} insulin, and 0.1 mg mL^{-1} cholera enterotoxin (Sigma–Aldrich, Milan, Italy). MDA-MB-231 human breast cancer cells, known as triple-negative cells (i.e., not overexpressing human epidermal growth factor receptor 2 (HER2), estrogen and progesterone receptors), were cultured in DMEM/F12, supplemented with 5% FBS, 1% L-glutamine and 100 U mL^{-1} penicillin/streptomycin. Cells were maintained at 37 °C in a humidified atmosphere of 95% air and 5% CO_2 and periodically screened for contamination.[44] Thalidomide or its analogues were dissolved in dimethyl sulfoxide (DMSO; Sigma, St. Louis, MO, USA) and opportunely diluted in DMEM/F12 medium to obtain working concentrations.

Cell viability. MDA-MB-231 and MCF-7 cells were grown in complete medium, and before being treated, they were starved in serum-free medium for 24 h, to allow cell-cycle synchronization. Cells were then grown in phenol-red-free medium supplemented with 1% dextran-coated charcoal (DCC)-treated FBS. Cells were treated with increasing concentrations (1, 5, 10, 25, 50, 100, and 500 μM) of each compound for 72 h. Untreated cells were supplemented with DMSO (final concentration 0.1%) and used as a control.[45] Cell viability was assessed using the 3-(4,5-dimethylthiazol-2-yl)-2,5-diphenyltetrazolium bromide reagent (MTT), according to the manufacturer's protocol (Sigma–Aldrich, Milan, Italy), as previously described.[46] For each sample, mean absorbance, measured at 570 nm, was expressed as a percentage of the control and plotted versus drug concentration to determine the IC_{50} values (i.e., drug concentrations able to decrease cell viability by 50% with respect to control) for each cell line, using GraphPad Prism 5 software (GraphPad Inc., San Diego, CA, USA). Mean values and standard deviations (SD) of three independent experiments carried out in triplicate and are shown.

Wound-healing assay. MCF-7 and MDA-MB-231 cells were plated on six-well plates and cultured in full medium to produce confluent monolayers. They were wounded in a line using a standard 200-μL sterile pipette tip, then washed with phosphate-buffered saline (PBS) to remove cell debris before incubation with various concentrations of each compound at its IC_{50} value, as indicated in Table 1. Images at time zero ($t = 0$ h) were acquired to record the initial area of the wound, and the recovery of the wounded monolayer due to cell migration toward the scratched area was estimated at 48 and 72 h ($t = \Delta h$). Images were captured using an inverted microscope equipped with digital camera (Leica DM6000). The migration of cells toward the wounds was expressed as percentage of wound closure [Eq. (1)]:

$$\text{wound closure } [\%] = [(At_0 - At_{\Delta h}) \times (At_0)^{-1}] \times 100\,\% \quad (1)$$

for which At_0 is the area of wound measured immediately after scratching, and $At_{\Delta h}$ is the area of wound measured 48 or 72 h after scratching. Vehicle-treated cells were used as a control. The collected images were analyzed with Leica Application Suite X (LAS X) software. Each experiment was performed three times, and each treatment was conducted in three replicates. Representative images are shown.

TUNEL assay. Apoptosis was detected by the TUNEL assay, according to the guidelines of the manufacturer (CF™488A TUNEL Assay Apoptosis Detection Kit, Biotium, Hayward, CA, USA), with some modifications.[47] In brief, cells were grown on glass coverslips. After treatment, they were washed three times with PBS, then methanol-fixed at −20 °C for 15 min. Fixed cells were washed three times with 0.01% (*v/v*) Triton X-100 in PBS and incubated with 100 μL TUNEL equilibration buffer for 5 min; this was then removed, and 50 μL TUNEL reaction mixture containing 1 μL terminal deoxynucleotidyl transferase (TdT) was added to each sample and incubated in a dark and humidified chamber for 2 h at 37 °C. Samples were washed three times with ice-cold PBS containing 0.1% Triton X-100 and 5 mg mL^{-1} bovine serum albumin (BSA). DAPI (0.2 μg mL^{-1}) counterstain was performed for 10 min at 37 °C under dark and humidified conditions. Cells were then washed three times with cold PBS, adding one drop of mounting solution, then they were observed and imaged under a fluorescence microscope (Leica DM6000; 20× magnification) with excitation/emission wavelength maxima of 490 nm/515 nm (CF™488A) or 350 nm/460 nm (DAPI). Images are representative of three independent experiments.

Immunofluorescence. For immunocytochemistry, cells were grown on coverslips in full media, then serum-starved for 24 h for the indicated time with examined compounds. Then they were PBS-washed and fixed with cold methanol (15 min/−20 °C) and washed three times (10 min/room temperature) with cold PBS containing 0.01% Triton X-100. After incubation (30 min/room temperature) with blocking solution (PBS, 2% BSA), they were incubated with primary antibodies diluted in blocking solution (4 °C/overnight). The primary antibody raised against E-cadherin (4065) and the antibody raised against vimentin (3932) were purchased from Cell Signaling (Cell Signaling technology, Milan, Italy) and both used at 1:100 dilution; anti-TNFα (52B83) and anti-VEGF (A-20), acquired from Santa Cruz Biotechnology Inc. (Santa Cruz, CA, USA), were used at 1:50 and 1:100 dilutions, respectively. Furthermore, the purified mouse anti-cytochrome *c* antibody (556433) was purchased from BD Biosciences and used at 1:100 dilution. Coverslips were then washed three times with PBS, then fixed cells were incubated with the secondary antibodies Alexa Fluor® 568 conjugate goat-anti-mouse or Alexa Fluor® 488 conjugate goat-anti-rabbit (both used at 1:500 dilution and acquired from Thermo Fisher Scientific, MA, USA). Nuclei were stained using DAPI (Sigma) for 10 min at a concentration of 0.2 μg mL^{-1} then washed three times with PBS. Fluorescence was detected by fluorescence microscopy (Leica

DM 6000). LAS-X software was used to acquire and process all images.[48]

Statistical analysis: Data were analyzed for statistical significance ($p < 0.001$) using one-way ANOVA followed by Dunnett's test performed by GraphPad Prism 5. Standard deviations (SD) are shown.

Abbreviations

ANOVA, analysis of variance; DAPI, 2-(4-amidinophenyl)-6-indolecarbamidine dihydrochloride; DMEM/F12, Dulbecco's modified Eagle's medium F12; EMT, epithelial–mesenchymal transition; FBS, fetal bovine serum; IIDQ, 2-isobutoxy-1-isobutoxycarbonyl-1,2-diihydroquinoline; MCF-7, Michigan Cancer Foundation-7; MCF-10A, Michigan Cancer Foundation-10A; MDA-MB-231, M.D. Anderson Metastatic Breast-231; MTT, 3-(4,5-dimethylthiazol-2-yl)-2,5-diphenyltetrazolium bromide; TNFα, tumor necrosis factor α; TUNEL, terminal deoxynucleotidyl transferase dUTP nick end labeling; VEGF, vascular endothelial growth factor.

Acknowledgements

This work was supported by MIUR (to M.S.S.). We thank Dr. Noemi Muià for her technical support.

Keywords: angiogenesis · antitumor activity · apoptosis · thalidomide · TNFα

[1] N. Vargesson, *Birth Defects Res. Part C* **2015**, *105*, 140 – 156.
[2] J. H. Kim, A. R. Scialli, *Toxicol. Sci.* **2011**, *122*, 1 – 6.
[3] J. J. Wu, D. B. Huang, K. R. Pang, S. Hsu, S. K. Tyring, *Br. J. Dermatol.* **2005**, *153*, 254 – 273.
[4] X. Wang, Y. Li, X. Yan, *Biomed. Res. Int.* **2016**, *2016*, 6848902.
[5] B. Y. A. El-Aarag, T. Kasai, M. A. H. Zahran, N. I. Zakhary, T. Shigehiro, S. C. Sekhar, H. S. Agwa, A. Mizutani, H. Murakami, H. Kakuta, M. Seno, *Int. Immunopharmacol.* **2014**, *21*, 283 – 292.
[6] M. Simon, B. Pariente, J. Lambert, J. Cosnes, Y. Bouhnik, P. Marteau, M. Allez, J. F. Colombel, J. M. Gornet, *Clin. Gastroenterol. Hepatol.* **2016**, *14*, 966 – 972.e2.
[7] P. Charles, C. Richaud, S. Beley, L. Bodard, M. Simon, *J. Clin. Virol.* **2016**, *78*, 12 – 13.
[8] A. Caruso, D. Iacopetta, F. Puoci, A. R. Cappello, C. Saturnino, M. S. Sinicropi, *Mini-Rev. Med. Chem.* **2016**, *16*, 630 – 643.
[9] D. Iacopetta, Y. Rechoum, S. A. Fuqua, *Drug Discovery Today Dis. Mech.* **2012**, *9*, e19 – e27.
[10] R. G. Jones, C. B. Thompson, *Genes Dev.* **2009**, *23*, 537 – 548.
[11] R. J. D'Amato, M. S. Loughnan, E. Flynn, J. Folkman, *Proc. Natl. Acad. Sci. USA* **1994**, *91*, 4082 – 4085.
[12] P. Carmeliet, *Oncology* **2005**, *69*, 4 – 10.
[13] X. Wang, Y. Lin, *Acta Pharmacol. Sin.* **2008**, *29*, 1275 – 1288.
[14] C. Chaulet, C. Croix, D. Alagille, S. Normand, A. Delwail, L. Favot, J. C. Lecron, M. C. Viaud-Massuard, *Bioorg. Med. Chem. Lett.* **2011**, *21*, 1019 – 1022.
[15] G. W. Muller, L. G. Corral, M. G. Shire, H. Wang, A. Moreira, G. Kaplan, D. I. Stirling, *J. Med. Chem.* **1996**, *39*, 3238 – 3240.
[16] G. W. Muller, M. G. Shire, L. M. Wong, L. G. Corral, R. T. Patterson, Y. Chen, D. I. Stirling, *Bioorg. Med. Chem.* **1998**, *8*, 2669 – 2674.
[17] M. Gütschow, T. Hecker, A. Thiele, S. Hauschildt, K. Eger, *Bioorg. Med. Chem.* **2001**, *9*, 1059 – 1065.
[18] E. R. Lepper, S. S. W. Ng, M. Gütschow, M. Weiss, S. Hauschildt, T. K. Hecker, F. A. Luzzio, K. Eger, W. D. Figg, *J. Med. Chem.* **2004**, *47*, 2219 – 2227.
[19] H. Arai, A. Furusu, T. Nishino, Y. Obata, Y. Nakazawa, M. Nakazawa, M. Hirose, K. Abe, T. Koji, S. Kohno, *Acta Histochem. Cytochem.* **2011**, *44*, 51 – 60.
[20] M. A. Huber, N. Kraut, H. Beug, *Curr. Opin. Cell Biol.* **2005**, *17*, 548 – 558.
[21] A. J. Trimboli, K. Fukino, A. de Bruin, G. Wei, L. Shen, S. M. Tanner, N. Creasap, T. J. Rosol, M. L. Robinson, C. Eng, M. C. Ostrowski, G. Leone, *Cancer Res.* **2008**, *68*, 937 – 945.
[22] A. Catalano, R. Luciani, A. Carocci, D. Cortesi, C. Pozzi, C. Borsari, S. Ferrari, S. Mangani, *Eur. J. Med. Chem.* **2016**, *123*, 649 – 664.
[23] C. Lamanna, A. Catalano, A. Carocci, A. Di Mola, C. Franchini, V. Tortorella, P. M. Vanderheyden, M. S. Sinicropi, K. A. Watson, S. Sciabola, *ChemMedChem* **2007**, *2*, 1298 – 1310.
[24] A. Carocci, G. Lentini, A. Catalano, M. M. Cavalluzzi, C. Bruno, M. Muraglia, N. A. Colabufo, N. Galeotti, F. Corbo, R. Matucci, C. Ghelardini, C. Franchini, *ChemMedChem* **2010**, *5*, 696 – 704.
[25] C. F. Bigge, S. J. Hays, P. M. Novak, J. T. Drummond, G. Johnson, T. P. Bobovski, *Tetrahedron Lett.* **1989**, *30*, 5193 – 5196.
[26] A. Catalano, A. Carocci, F. Corbo, C. Franchini, M. Muraglia, A. Scilimati, M. De Bellis, A. De Luca, D. Conte Camerino, M. S. Sinicropi, V. Tortorella, *Eur. J. Med. Chem.* **2008**, *43*, 2535 – 2540.
[27] A. Catalano, A. Carocci, G. Lentini, A. Di Mola, C. Bruno, C. Franchini, *J. Heterocycl. Chem.* **2011**, *48*, 261 – 266.
[28] M. Muraglia, M. De Bellis, A. Catalano, A. Carocci, C. Franchini, A. Carrieri, C. Fortugno, C. Bertucci, J. F. Desaphy, A. De Luca, D. C. Camerino, F. Corbo, *J. Med. Chem.* **2014**, *57*, 2589 – 2600.
[29] A. Catalano, A. Carocci, M. M. Cavalluzzi, A. Di Mola, G. Lentini, A. Lovece, A. Dipalma, T. Costanza, J. F. Desaphy, D. Conte Camerino, C. Franchini, *Arch. Pharm. Chem. Life Sci.* **2010**, *343*, 325 – 332.
[30] S. Miyano, K. Sumoto, F. Satoh, K. Shima, M. Hayashimatsu, M. Morita, K. Aisaka, T. Noguchi, *J. Med. Chem.* **1985**, *28*, 714 – 717.
[31] A. Catalano, R. Budriesi, C. Bruno, A. Di Mola, I. Defrenza, M. M. Cavalluzzi, M. Micucci, A. Carocci, C. Franchini, G. Lentini, *Eur. J. Med. Chem.* **2013**, *65*, 511 – 516.
[32] G. Palma, G. Frasci, A. Chirico, E. Esposito, C. Siani, C. Saturnino, C. Arra, G. Ciliberto, A. Giordano, M. D'Aiuto, *Oncotarget* **2015**, *6*, 26560 – 26574.
[33] E. Sirignano, A. Pisano, A. Caruso, C. Saturnino, M. S. Sinicropi, R. Lappano, A. Botta, D. Iacopetta, M. Maggiolini, P. Longo, *Anti-Cancer Agents Med. Chem.* **2015**, *15*, 468 – 474.
[34] O. I. Parisi, C. Morelli, F. Puoci, C. Saturnino, A. Caruso, D. Sisci, G. E. Trombino, N. Picci, M. S. Sinicropi, *J. Mater. Chem. B* **2014**, *2*, 6619 – 6625.
[35] A. L. Moreira, E. P. Sampaio, A. Zmuidzinas, P. Frindt, K. A. Smith, G. Kaplan, *J. Exp. Med.* **1993**, *177*, 1675 – 1680.
[36] J. C. Yang, G. A. Cortopassi, *Free Radicals Biol. Med.* **1998**, *24*, 624 – 631.
[37] P. Rizza, M. Pellegrino, A. Caruso, D. Iacopetta, M. S. Sinicropi, S. Rault, J. C. Lancelot, H. El-Kashef, A. Lesnard, C. Rochais, P. Dallemagne, C. Saturnino, F. Giordano, S. Catalano, S. Ando, *Eur. J. Med. Chem.* **2016**, *107*, 275 – 287.
[38] R. Singhai, V. W. Patil, S. R. Jaiswal, S. D. Patil, M. B. Tayade, A. V. Patil, *North Am. J. Med. Sci.* **2011**, *3*, 227 – 233.
[39] J. Komorowski, H. Jerczynska, A. Siejka, P. Baranska, H. Lawnicka, Z. Pawlowska, H. Stepien, *Life Sci.* **2006**, *78*, 2558 – 2563.
[40] T. H. Lee, S. Seng, M. Sekine, C. Hinton, Y. Fu, H. K. Avraham, S. Avraham, *PLoS Med.* **2007**, *4*, e186.
[41] W. L. Li, G. A. Keller, *J. Cell Sci.* **2000**, *113*, 1525 – 1534.
[42] A. Carocci, A. Catalano, C. Bruno, G. Lentini, C. Franchini, M. De Bellis, A. De Luca, D. Conte Camerino, *Chirality* **2010**, *22*, 299 – 307.
[43] A. Chimento, M. Sala, I. M. Gomez-Monterrey, S. Musella, A. Bertamino, A. Caruso, M. S. Sinicropi, R. Sirianni, F. Puoci, O. I. Parisi, C. Campana, E. Martire, E. Novellino, C. Saturnino, P. Campiglia, V. Pezzi, *Bioorg. Med. Chem. Lett.* **2013**, *23*, 6401 – 6405.
[44] E. Sirignano, C. Saturnino, A. Botta, M. S. Sinicropi, A. Caruso, A. Pisano, R. Lappano, M. Maggiolini, P. Longo, *Bioorg. Med. Chem. Lett.* **2013**, *23*, 3458 – 3462.
[45] M. S. Sinicropi, A. Caruso, F. Conforti, M. Marrelli, H. El Kashef, J. C. Lancelot, S. Rault, G. A. Statti, F. Menichini, *J. Enzyme Inhib. Med. Chem.* **2009**, *24*, 1148 – 1153.
[46] A. Carocci, A. Catalano, C. Bruno, A. Lovece, M. G. Roselli, M. M. Cavalluzzi, F. De Santis, A. De Palma, M. R. Rusciano, M. Illario, C. Franchini, G. Lentini, *Bioorg. Med. Chem.* **2013**, *21*, 847 – 851.
[47] D. Iacopetta, C. Rosano, F. Puoci, O. I. Parisi, C. Saturnino, A. Caruso, P. Longo, J. Ceramella, A. Malzert-Fréon, P. Dallemagne, S. Rault, M. S. Sinicropi, *Eur. J. Pharm. Sci.* **2017**, *96*, 263 – 272.

[48] D. Iacopetta, R. Lappano, A. R. Cappello, M. Madeo, E. M. De Francesco, A. Santoro, R. Curcio, L. Capobianco, V. Pezzi, M. Maggiolini, V. Dolce, *Breast Cancer Res. Treat.* **2010**, *122*, 755 – 764.

Manuscript received: December 14, 2016
Revised: January 16, 2017

Accepted Article published: ■■ ■■, 0000

Final Article published: ■■ ■■, 0000

Thalidomide redirected! Compounds **3** and **8** act on different key points of the tumorigenesis process by drastically reducing the migration of breast cancer cells, through the regulation of vimentin and E-cadherin and by diminishing the intracellular biosynthesis of vascular endothelial growth factor (VEGF).

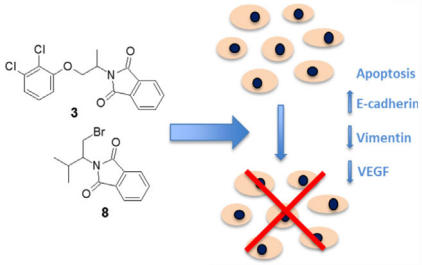

D. Iacopetta, A. Carocci, M. S. Sinicropi, A. Catalano,* G. Lentini, J. Ceramella, R. Curcio, M. C. Caroleo*

■■ – ■■

Old Drug Scaffold, New Activity: Thalidomide-Correlated Compounds Exert Different Effects on Breast Cancer Cell Growth and Progression

#Thalidomide analogues @UniCalPortale @UniBaIt fight #breastcancer by anti-#angiogenesis SPACE RESERVED FOR IMAGE AND LINK

Share your work on social media! *ChemMedChem* has added Twitter as a means to promote your article. Twitter is an online microblogging service that enables its users to send and read text-based messages of up to 140 characters, known as "tweets". Please check the pre-written tweet in the galley proofs for accuracy. Should you or your institute have a Twitter account, please let us know the appropriate username (i.e., @accountname), and we will do our best to include this information in the tweet. This tweet will be posted to the journal's Twitter account @ChemMedChem (follow us!) upon online publication of your article, and we recommended you to repost ("retweet") it to alert other researchers about your publication.

Please check that the ORCID identifiers listed below are correct. We encourage all authors to provide an ORCID identifier for each coauthor. ORCID is a registry that provides researchers with a unique digital identifier. Some funding agencies recommend or even require the inclusion of ORCID IDs in all published articles, and authors should consult their funding agency guidelines for details. Registration is easy and free; for further information, see http://orcid.org/.

Dr. Domenico Iacopetta
Dr. Alessia Carocci
Prof. Maria Stefania Sinicropi
Dr. Alessia Catalano
Prof. Giovanni Lentini
Dr. Jessica Ceramella
Dr. Rosita Curcio
Prof. Maria Cristina Caroleo

These are not the final page numbers! ↗↗